

Application of GaAs Discrete p-HEMTs in Low Cost Phase Shifters and QPSK Modulators

Stanimir D. Kamenopolsky

The application of a discrete pseudomorphic high electron mobility transistor (p-HEMT) as a grounded switch allows for the development of low cost phase shifters and phase modulators operating in a Ku band. This fills the gap in the development of phase control devices comprising p-i-n diodes and microwave monolithic integrated circuits (MMICs). This paper describes a discrete p-HEMT characterization and modeling in switching mode as well as the development of a low-cost four-bit phase shifter and direct quadrature phase shift keying (QPSK) modulator. The developed devices operate in a Ku band with parameters comparable to commercially available MMIC counterparts. Both of them are CMOS compatible and have no power consumption. The parameters of the QPSK modulator are very close to the requirements of available standards for satellite earth stations.

Keywords: Phase shifter, QPSK modulator, p-HEMT modeling, cold FET measurements, Ku band.

I. Introduction

State of the art mobile satellite communications are closely related to the application of phase control devices such as phase shifters and phase modulators as a part of transmit- and receive-phased array antennas [1], [2]. In the past, the development of high-performance discrete and hybrid phase shifters and modulators operating in X and Ku bands was based on beam lead *p-i-n* diodes used as a main switching component [3]-[5]. Beam lead *p-i-n* diodes have excellent microwave properties such as low resistance in low impedance states and low capacitance in high impedance states. Each of these properties makes the devices suitable for broadband operation. Despite their microwave advantages, *p-i-n* diodes do have some drawbacks: a relatively high power consumption and a related complicated driving circuit, a low switching speed, and a relatively high price compared to the price of other microwave discrete components. All of these limit their application in low-cost microwave terminals using a large number of switching components.

Nowadays, phase control devices are built mainly as microwave monolithic integrated circuits (MMICs) using metal semiconductor field effect transistors or pseudomorphic high electron mobility transistors (p-HEMT) implemented on a GaAs substrate [6]-[9]. The application of an MMIC yields a compact and multifunctional design, making the final product reliable and well performing. Nevertheless, the development of a custom-designed MMIC for a specific application and frequency band is a long-term procedure, which requires a large financial investment and often needs at least two iterations. Moreover, a GaAs substrate has a high dielectric loss of $\text{tg}\delta = 6\text{E-}3$, which dictates larger insertion losses of the passive devices. In more cases, MMIC control devices require the

Manuscript received Dec. 2, 2003; revised Mar. 17, 2004.

Stanimir D. Kamenopolsky (phone: +359 2 962 1285, email: kamenopolsky_s@skygate.bg) is with RF Design Team, Sky Gate Ltd., Sofia, Bulgaria.

integration of a digital circuitry, which additionally complicates the design and increases the power consumption.

An interesting alternative filling the gap between the application of *p-i-n* diodes and MMICs in phase control devices is a discrete low-cost GaAs p-HEMT. This device is normally used in low-noise down converters as either an amplifier or as an active mixer. A precise measurement of cold p-HEMT two-state S-parameters allows its application as a grounded switch in X and Ku bands. A discrete p-HEMT gives an advantage to developed devices in terms of design time, price, insertion loss, adjustability, and power consumption. The application of a discrete p-HEMT suffers from a relatively large occupied area compared to its MMIC counterparts. Therefore, devices comprising it are suitable for building engineering models, verifying the design concept before investing in the development of the final product.

In [10] and [11], I described a five-bit phase shifter employing a discrete p-HEMT. The device operates in the whole satellite band from 10.7 to 12.75 GHz and uses a novel circuit for implementing the less significant bit. The phase shifter has 6-dB insertion losses with a ± 1.4 -dB maximum variation and a 3°-averaged RMS phase error. This device occupies a relatively large area of 12 cm \times 2.3 cm (27.6 cm²) and is difficult for implementation in phased array antennas.

This paper describes a discrete GaAs p-HEMT characterization and modeling as well as the development of a discrete four-bit phase shifter with an almost triple reduction in size (10 cm²), a 1.5-dB improved insertion loss, and a 2°-averaged RMS phase error than previously reported in [10]. The application of this discrete p-HEMT in a direct quadrature phase shift keying (QPSK) modulator operating in X and Ku bands is also presented in this paper.

II. Discrete p-HEMT Characterization and Modeling

The application of a discrete p-HEMT as a grounded switch in a Ku band is not a common practice, and therefore manufacturers rarely supply the S-parameters of such devices in switching mode. On the other hand, the provided parameters of most nonlinear models for discrete field effect transistors (FETs) are not extended to drain-source voltages of 0 V. All of these circumstances dictate the need for measuring the cold FET two-state parameters. For application as a grounded switch, a discrete p-HEMT (NEC, part number NE3210S01) is chosen. The device is placed in a low-cost plastic package and has two source terminals. For this measurement, a true-reflect-line (TRL) calibration technique is applied as the most promising for yielding an accurate result, presenting the discrete p-HEMT in a real operational environment. The test fixture illustrated in Fig. 1 is used for the TRL calibration and measurement.

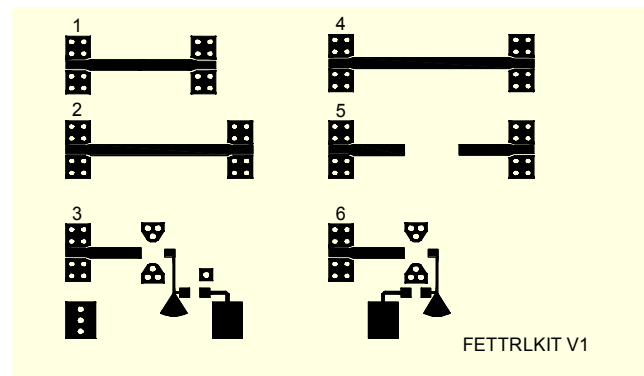


Fig. 1. TRL measurement test fixture from [10].

This fixture is built on an RO4003 substrate with a thickness of $h=0.51$ mm. The measurement structures 1, 2, and 5 are used for TRL calibration whereas structures 3 and 6 are for device characterization. Calibration standard 1 is a true line, 2 is a line with a 20-ps additional time delay, and 5 is a high-reflective open-end standard. Structure 4 is optional and provides broadband calibration. This calibration is made in a 10 to 13 GHz frequency band, and the reference plane is set by the true standard. During the measurement process, the drain-source voltage was 0 V, and control voltages of 0 V and -2 V were applied between the gate and the source of the transistor through a high impedance network connected to the gate. This measurement is accomplished using an HP8510B vector network analyzer in a 10 to 13 GHz frequency range. The obtained two-state S-parameters are shown in Fig. 2.

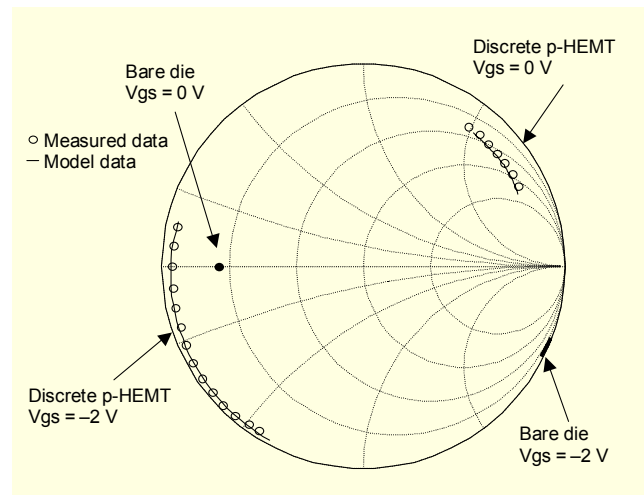


Fig. 2. Reflection parameters of measured (from [10]) and modeled p-HEMT in a 10- to 13-GHz frequency range.

The two impedance states of the device are clearly distinguished and are almost 180° apart. They are opposite on the impedance chart due to the package parasitic components and have a noticeable frequency dispersion. A general property

of microwave switches is their quality factor, \hat{Q} , introduced by Kurokawa and Schlosser, which is calculated by measured one-port parameters using the following equation:

$$\hat{Q}^2 = \frac{4|\Gamma_1 - \Gamma_2|^2}{(1 - |\Gamma_1|^2)(1 - |\Gamma_2|^2)}, \quad (1)$$

where Γ_1 and Γ_2 are measured one-port two-state reflection coefficients. The calculated quality factor \hat{Q}^2 in a frequency band of 10 to 13 GHz is depicted in Fig. 3.

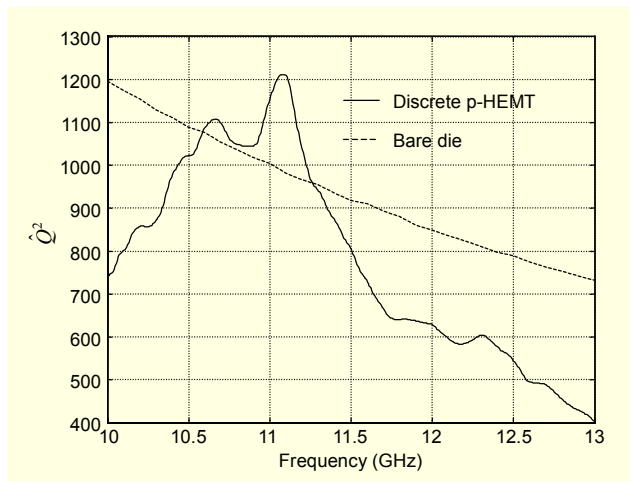


Fig. 3. Quality factor \hat{Q}^2 of a discrete p-HEMT and bare die in a 10- to 13-GHz frequency range.

The quality factor of a discrete p-HEMT is not a monotone function because of the parasitic components associated with the package. These components cause an increase of the quality factor to values above 1000 in a frequency range between 10.4 and 11.22 GHz, which is considered an advantage and will result in better switching properties. The average value of \hat{Q}^2 in the measured frequency band is 781. In order to evaluate the influence of the package upon the switching properties of the p-HEMT, an equivalent circuit of a discrete p-HEMT is developed based on the measurement results, manufacturer information about the device, a microscopic dimensions measurement, and observation of the uncovered device. An investigated discrete p-HEMT is manufactured on a 140- μm thick GaAs substrate with four gate fingers, having a total width of 160 μm and a length of less than 0.2 μm . The device is assembled in a low-cost plastic package with four golden-plated leads with a length of 1.4 mm and a width of 0.5 mm. The p-HEMT die is connected to the leads by a golden 25- μm wire bond with an average length of 500 μm . Two bonding wires are used for source terminals. Equivalent circuits of the p-HEMT die and packaged device are illustrated in Fig. 4. The table in the same figure presents the component values for two gate-source voltages, 0 V and -2 V.

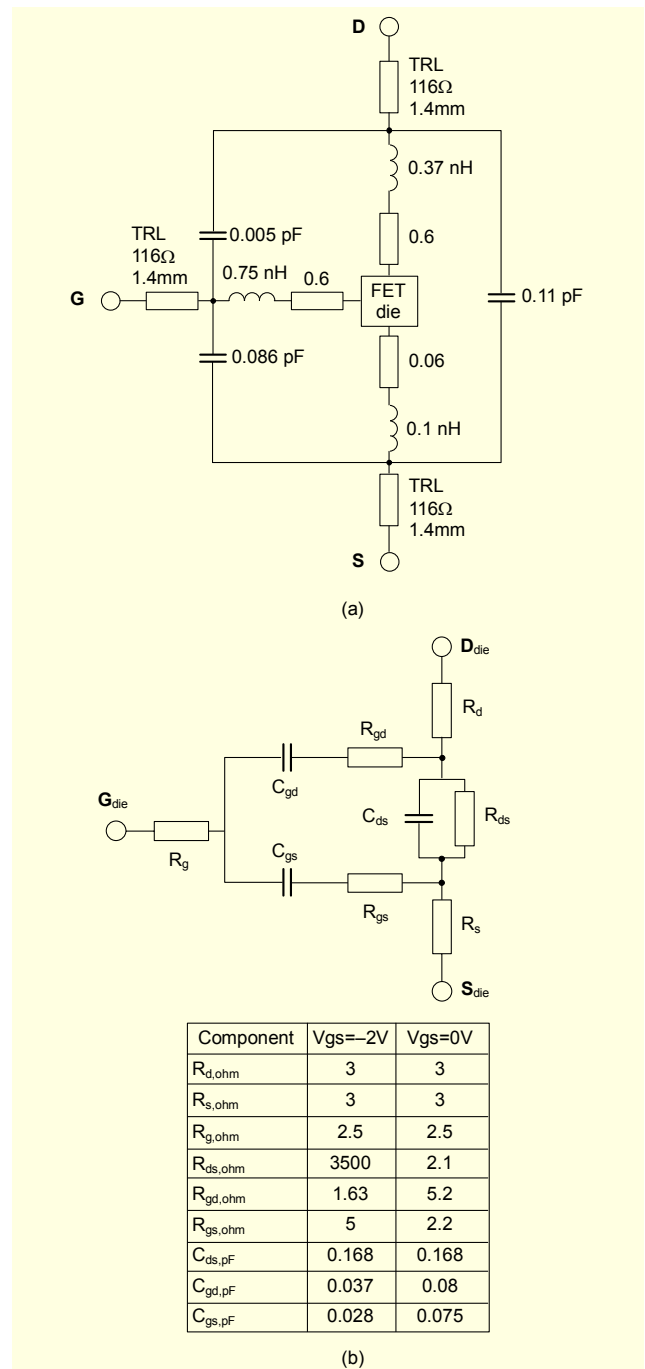


Fig. 4. Model of a discrete p-HEMT in a frequency range from 10- to 13-GHz: (a) package model, (b) p-HEMT die model. The substrate thickness, h , is 140 μm ; the total width of the gate, W , is 160 μm ; the gate length, L , is less than 0.2 μm ; and the number of gate fingers, N , is 4.

The initial component values are taken from the published data for a cold FET-equivalent circuit [4], [7], and the final component values are obtained after a CAD optimization of the initial model values in order to fit the measured data. An optimization and model simulation is done by means of a

commercial circuit simulator, Serenade 8.7. The presented model has two parts, a description of the bare die and a description of the package. The two-state parameters of a modeled discrete p-HEMT in a 10- to 13-GHz range are shown in Fig. 2. They are in close agreement with the measured results. The same figure presents the data for a modeled p-HEMT die, which shows a small frequency dispersion in the investigated band and the correct location of two impedance states on the Smith chart. The predicted quality factor of the p-HEMT die is plotted in Fig. 3 and shows that it is a monotone function with an average value of 935. It can be concluded that the device package causes a frequency dispersion and quality factor degradation of the p-HEMT die used as a grounded switch. In spite of these package effects, the measured properties of a discrete p-HEMT are good enough for the development of phase shifters and modulators with decent parameters, which in some cases even compete with their market-available monolithic counterparts.

III. Four-Bit Phase Shifter

The design of phase shifters is a straightforward procedure well described in the literature [3]–[7], [10] and [11]. The required preliminary design information is contained in the general phase shifter parameters and the switching component two-state scattering parameters. The designed phase shifter will be used in a receiving DBS phased-array antenna that operates in a 12.2- to 12.7-GHz frequency band. The device will be the main steering component, providing phase control of the received signal over a 0° to 337.5° phase range in 22.5° phase steps. The chosen substrate material is RO4003 with a thickness of $h=0.51$ mm and allows the implementation of a large variety of characteristic impedances. It is chosen for the construction of 22.5° and 45° phase-shifting bits using a loaded line configuration, whereas 90° and 180° phase-shifting bits utilize a hybrid coupled reflection type circuit. The loaded line circuits use impedance scaling in shunting branches for two reasons: to maintain the required admittances and to facilitate the soldering of a discrete p-HEMT. The relative bandwidth for a DBS band is about 5%, and therefore single-section branch-line couplers are used in reflection type circuits. The layout of a discrete four-bit phase shifter is illustrated in Fig. 5. The phase shifter comprises eight discrete p-HEMTs and eight resistors for CMOS level shifting. The microwave part of the phase shifter is placed on a $10\text{ cm} \times 1\text{ cm}$ (10 cm^2) area on the topside of the substrate. The applied driving circuitry described in [10] is located on the backside of the substrate to make a compact design. The control of the phase shifter is CMOS-compatible (5 V) and requires only a -5 V external power supply and GND. The driving circuit is a resistive level shifter, which

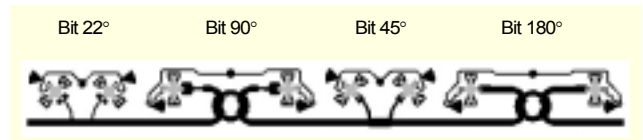


Fig. 5. Layout of a four-bit phase shifter implemented on an $h=0.51$ mm RO4003 substrate.

Table 1. Four-bit phase shifter general parameters (simulation & measurement).

Parameters	Unit	Sim.	Meas.
Average RMS phase error	Deg.	2	2
Maximum phase error	Deg.	9	8
Average insertion loss	dB	4.15	4.5
Insertion loss deviation	dB	± 1.2	± 1.4
Maximum input return loss	dB	14.5	13
Maximum output return loss	dB	15.1	15.4
Average group delay	ns	1.2	1.2
Group delay deviation	ns	± 0.59	± 0.35
Setting time	ns	-	< 70
Frequency band	GHz	12.2 – 12.8	

provides FET's own switching voltages of 0 and -2.5 V . The impedance of the driving inputs is mainly determined by the values of the level shifting resistors and can be kept relatively high. With the values of those resistors at $10\text{ k}\Omega$, the phase shifter was successfully driven with a data speed of 14 Mb/s .

The measurements are made by means of an HP8720ES vector network analyzer with SMA terminations on the device. The frequency responses of the phase shifter in a 12.2- to 12.8-GHz frequency range are depicted in Figs. 6 and 7. Figure 6 presents the relative phase delay of the four-bit phase shifter, where the first state of the device is adopted as a reference state—all FETs are on. The transmission and reflection coefficients are depicted in Fig. 7. A general phase shifter is simulated and measured parameters are summarized in Table 1. The measured values are close to the simulated ones and the differences are mainly due to production tolerances, which in this particular case are $\pm 20\text{ }\mu\text{m}$ for the line widths. The measured phase shifter is also 50-MHz shifted in the upper frequency band. The simulated frequency range was 12.15 to 12.75 GHz.

The phase shifter exhibits an average insertion loss of 4.5 dB with a maximum deviation of $\pm 1.4\text{ dB}$. The matching of the device is very good, and the input return loss has a worst-case value of 13 dB only at the edges of the frequency band of interest. The maximum phase error is 8° and the calculated

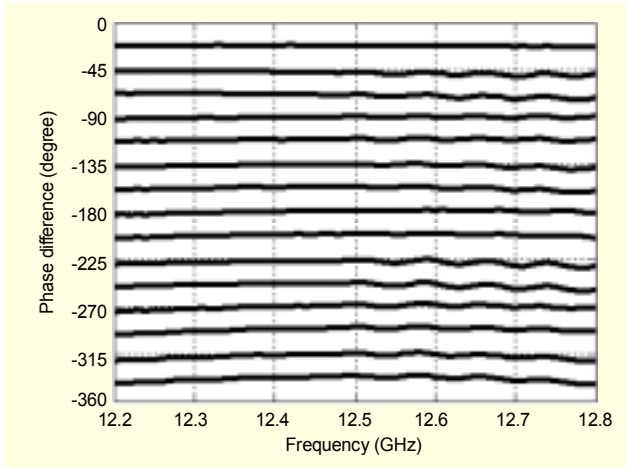


Fig. 6. Four-bit phase shifter relative phase delay for all 16 states.

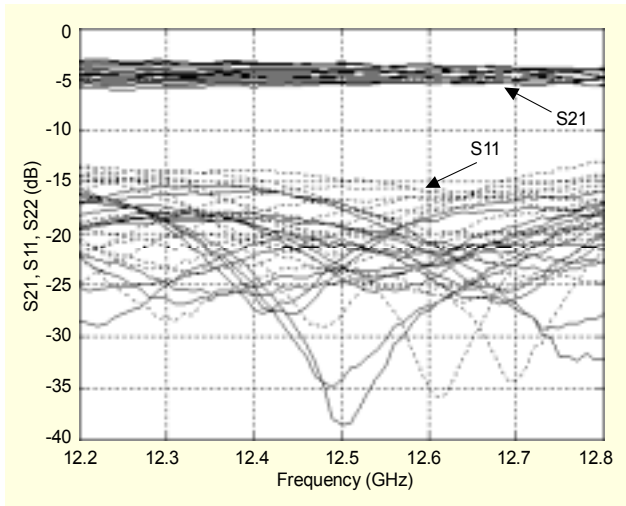


Fig. 7. Four-bit phase shifter insertion and return losses for all 16 states.

average RMS phase error for all states is 2° , which is appropriate for beam steering and polarization control in mobile DBS receiving terminals. The phase shifter has a true phase-delay response with a constant time delay of 1.2 ns for all 16 states with a maximum deviation of ± 0.35 ns. The setting time of the phase control device is better than 70 ns and could be further decreased by optimizing the values of the level shifting resistors. The performance of the MMIC counterpart without a package [13] operating in the same band is as follows: an insertion loss of 6 dB, a return loss of 15 dB, and a maximum phase error of 7° . Comparing the parameters of both devices we can see that they are almost identical even though the presented discrete phase shifter has a 1.5-dB better insertion loss. This difference will increase when the MMIC is packaged.

The achieved size reduction, a factor of 2.7 compared to the phase shifter in [10], is mainly due to the application of single-section branch-line couplers and the moving of the controlling

part on the backside of the substrate. Other advantages of this are a 1.5-dB reduced insertion loss and a better matching of 2 dB; the tradeoff is a reduced bandwidth, which in this particular case is sufficient. The addition of the fifth bit to the developed phase shifter will increase the losses to 4.7 dB and the size to $11.5 \text{ cm} \times 1 \text{ cm}$ (11.5 cm^2).

IV. Direct QPSK Modulator

The application of a direct modulation technique in a digital microwave radio makes some of the frequency translation blocks redundant and causes a cost reduction of the overall transmitting tract [8]. The presented QPSK modulator comprises two 180° phase-shifting bits, a Wilkinson divider, and a double-section branch-line coupler. The implemented phase shifting bits also use double-section branch-line couplers to accommodate a whole satellite TV band. All of the discrete parts used are four p-HEMTs and five resistors. The driving of the modulating inputs I and Q is CMOS-compatible and is the same as the driving of the described phase shifter. The QPSK modulator is placed on an RO4003 substrate with a dimension of $43 \text{ mm} \times 44 \text{ mm}$. The implemented layout is depicted in Fig. 8.

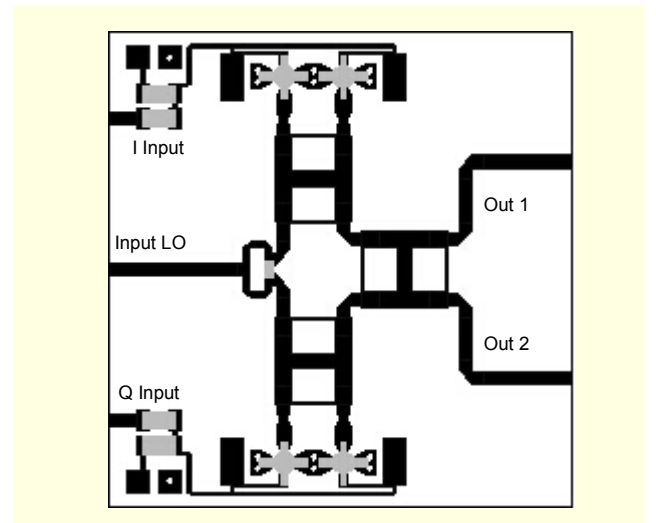


Fig. 8. Layout of a QPSK modulator implemented on an $h=0.51$ RO4003 substrate.

The theoretical prediction of the expected insertion loss of the QPSK modulator is made on the base of the losses in the whole QPSK signal chain expressed with

$$IL_{QPSK} = 3 + IL_{RB} + 2L_{SMA} + L_{In} + L_{Out} + 2L_H + L_W, \quad (2)$$

where IL_{QPSK} is the insertion loss of the QPSK modulator; IL_{RB} is the insertion loss of the reflection type phase shifting bit; L_{SMA} is the insertion loss in the SMA terminations (not included

Table 2. QPSK modulator loss factor values.

Loss factors	IL_{QPSK}	IL_{RB}	L_{SMA}	L_{In}	L_{Out}	L_H	L_W
Values (dB)	4.93	0.65	0.15	0.15	0.18	0.25	0.15

in Fig. 9) and coaxial to microstrip transition; L_{In} and L_{Out} are the insertion losses in the input/output microstrip feeding lines; and L_H and L_W are the insertion losses in the 3-dB double-section branch-line coupler and the Wilkinson divider. The constant term of 3 is due to the fact that the combined output signals in a QPSK modulator are 90° out of phase. Table 2 shows the summarized values of the losses of each component in (2).

The calculation for the insertion loss of 180° phase-shifting bit IL_{RB} is made by the help of (3) reported in [5] and uses the calculated quality factor of the discrete p-HEMT switch, $\hat{Q}^2 = 781$.

$$IL_{RB} = 20 \lg |\Gamma_{RL}|, \quad m^2 = \frac{8(1 - \cos \phi)}{\hat{Q}^2}, \quad (3)$$

$$|\Gamma_{RL}| = \left| \frac{m}{2} - \sqrt{1 + \frac{m^2}{4}} \right|,$$

where IL_{RB} is the insertion loss of the reflection type phase shifting bit; Γ_{RL} is the reflection coefficient of the reflective load; ϕ is the implemented phase shift—in this case 180° —and \hat{Q}^2 is the quality factor of the discrete p-HEMT. The calculated value for the insertion losses of the QPSK modulator is 4.93 dB, assuming the 180° phase-shifting bit has no parasitic amplitude variation. This is the condition when (3) is valid.

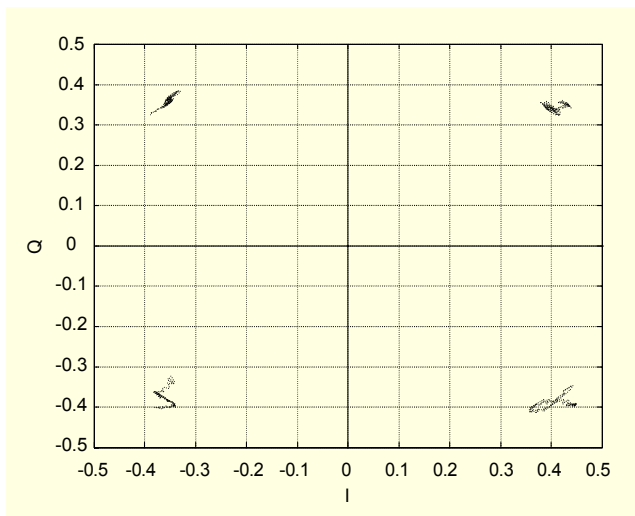


Fig. 9. Constellation of the signal states at the output of a QPSK modulator in a 10.6 to 12.8 GHz frequency range.

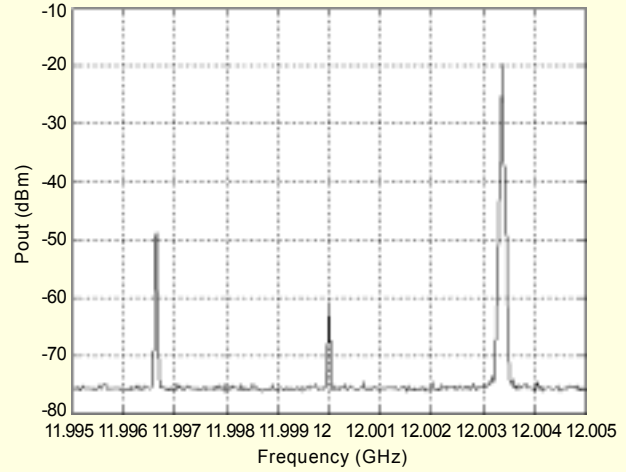


Fig. 10. Lower single-sideband rejection at the output of the QPSK modulator. Spectrum analyzer setting: CW = 12 GHz, Span=10 MHz, RB=10 kHz, VBW=10 kHz.

The phase and amplitude responses of the QPSK modulator are measured using an HP8720ES vector network analyzer.

The constellation of the signal in the device output in a 10.6- to 12.8-GHz frequency band is presented in Fig. 9.

The average measured insertion loss of the modulator is 5.5 dB, which is 0.57 dB higher than predicted. The reason for this is the bigger loss in the phase shifting bits, which are designed to accommodate a 2.2-GHz bandwidth. A tradeoff is made in the choice of the reflection coefficients of the reflective load, which increases the amplitude variation of the phase shifting bit output in order to assure phase accuracy in the broader bandwidth. A measure of the quality of QPSK modulators is their ability to reject a signal carrier and a one-side band in the spectrum of the output signal when I and Q modulating signals are 90° out of phase. Single-sideband suppression can be calculated with (4) reported in [14].

$$SSS = 10 \log \left[\frac{G^2 - 2G \cos \phi + 1}{G^2 + 2G \cos \phi + 1} \right], \quad (4)$$

where SSS is the single sideband suppression, G is an amplitude error, and ϕ is a phase error. The measured phase and amplitude errors of the modulator at 12 GHz for all states are 2.6° and 0.26 dB, which corresponds to single-sideband suppression of 31.2 dBc. The data for the carrier and sideband rejection—at 12 GHz for the carrier and 3.4 MHz for the I and Q modulating signals—are measured directly using an HP8593E spectrum analyzer. Spectrograms of the output signals are presented in Fig. 10. The carrier rejection is 40 dB and the single sideband suppression is 30 dB. This value is in close agreement with the calculated one. The QPSK modulator is also tested using a

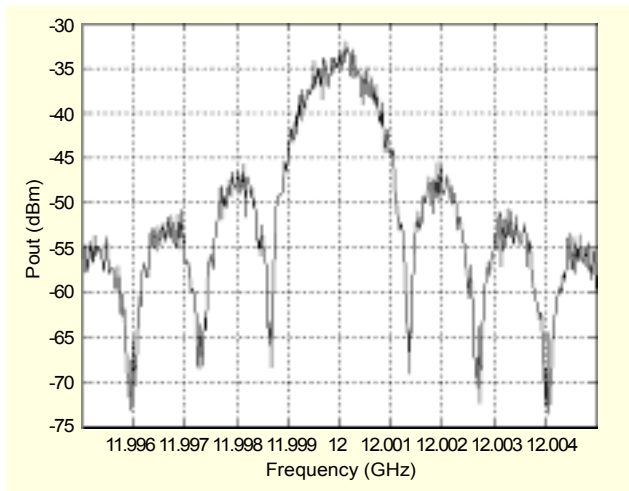


Fig. 11. Spectrogram of the signal at the output of the QPSK modulator at 12 GHz. Spectrum analyzer setting: CW = 12 GHz, Span=100 MHz, RB=300 kHz, VBW=100 kHz.

Table 3. QPSK modulator general parameters.

Parameters	Unit	Value
Average insertion loss	dB	5.5
RMS amplitude error	dB	0.4
RMS phase error	degree	3.2
Sideband suppression	dB	30
Carrier suppression	dB	40
RF input/output impedance	ohm	50
Modulation input impedance	ohm	5000
Modulation input level	V	CMOS (5)
Frequency band	GHz	10.6 – 12.8

pseudo-random code sequence with a speed of 14Mbits/s for the I and Q components. The obtained output spectrograms are depicted in Fig. 11, where the parasitic carrier rejection is well observed. The general QPSK modulator parameters are systemized in Table 3. These parameters are obtained after a small adjustment of the negative power supply to overcome the differences in the pinch-off voltages of the discrete p-HEMTs. Those broadband parameters are very close to the requirements of the Intelsat IESS-308 standard [15] for QPSK modulators in a satellite earth station.

V. Conclusion

Microwave signal processing frequently needs the application of phase shifters and phase modulators in terminals such as mobile phased array antennas. Those devices have not been

available on the market at a low cost for a long time. In most cases, this limits the development of terminals with a large number of phase-control devices for consumer applications where fast development, low cost, and low power consumption are of great importance. The application of a discrete p-HEMT in phase-control devices breaks this limit, where available space allows it. The described phase shifter was successfully implemented in commercial DBS terminals for mobile reception as a main steering and polarization control element. The QPSK modulator will be used in a terrestrial satellite simulator for the testing of receiving phased array antennas.

References

- [1] C.O. Adler, D.J. Alen, R.S. Carson, A.F. Morrison, M.E. Lavelle, E.D. Anderson et al, "Airborne Reception of Data and Direct Broadcast TV Using a Phased Array Antenna," *Proc. 2000 IEEE Int. Conf. on Phased Array Systems & Technology*, California, 2000, pp. 223–226.
- [2] S.A. Raby, R.Y. Shimoda, P.T. Heisen, D.E. Reimer, B.L. Blaser, G.R. Onorati, "Ku – Band Transmit Phased Array Antenna for Use in FSS Communication System," *Proc. 2000 IEEE Int. Conf. on Phased Array Systems & Technology*, California, 2000, pp. 227–230.
- [3] L.O. Francis and W.F. Hoffman, "Design of Digital Loaded Line Phase-Shift Networks for Microwave Thin-Film Applications," *IEEE Transactions on Microwave Theory and Techniques*, vol. MTT-16, no. 7, July 1968, pp. 462–468.
- [4] S.K. Koul and B. Bhat, *Microwave and Millimeter Wave Phase Shifters, Volume II: Semiconductor and Delay Line Phase Shifters*, 2nd ed., Artech House, 1991.
- [5] H.A. Atwater, "Impedance Transformations for the Generalized Reflection Modulator," *IEEE Transactions on Microwave Theory and Techniques*, vol. MTT-29, no. 3, Mar. 1981, pp. 229–234.
- [6] C. Andricos, I.J. Bahl, and E.L. Griffin, "C-Band 6 - Bit GaAs Monolithic Phase Shifter," *IEEE Transactions on Microwave Theory and Techniques*, vol. MTT-33, no. 12, Dec. 1985, pp. 1591–1596.
- [7] J.E. Penn, "A Broadband, Four-Bit, Ka-Band MMIC Phase Shifter" *Microwave J.*, vol. 44, no. 12, Dec. 2001, pp. 84–96.
- [8] A.E. Ashtiani, T. Gokdemir, G. Passiopoulos, A.A. Rezazadeh, S. Nam, and I.D. Robertson, "Miniaturized Low Cost 30 GHz Monolithic Balanced BPSK and Vector Modulators: Part I," *Microwave J.*, vol. 42, no. 3, Mar. 1999, pp. 100–104.
- [9] A.E. Ashtiani, T. Gokdemir, G. Passiopoulos, A.A. Rezazadeh, S. Nam, and I.D. Robertson, "Miniaturized Low Cost 30 GHz Monolithic Balanced BPSK and Vector Modulators: Part II," *Microwave J.*, vol. 42, no. 4, Apr. 1999, pp. 104–107.
- [10] S.D. Kamenopolsky, "Low Cost 5-Bit Phase Shifter for DBS Phased Array Antennas," *33rd European Microwave Conf.*, Oct. 2003, pp. 801–804.
- [11] S.D. Kamenopolsky, "Digitally Controlled Phase Shifter," Bulgarian Application for Patent 1 077 71, Apr. 30, 2003.

- [12] H.A. Atwater and R.W. Sudbury, "Use of Switching Q in the Design of FET Microwave Switches," *MTT-S Int. Microwave Symp. Digest*, June 1981, pp. 370–372.
- [13] J. Wallace, H. Redd, and R. Furlow, "Low Cost MMIC DBS Chip Sets for Phased Array Applications," *MTT-S Int. Microwave Symp. Digest*, vol. II, June 1999, pp. 677–680.
- [14] W.S. Djen, "Application Note AN 1892, SA900 I/Q Transmit Modulator for 1 GHz Application," Philips Semiconductor, Aug. 1997.
- [15] Intelsat, IESS-308 (Rev. 10), *Intelsat, Earth Station Standard*, 2001.



Stanimir D. Kamenopolsky received the MS degree in communications (with honors) from Technical University of Sofia, Bulgaria in 1995. From 1994 to 1997, he was with the satellite communication company Elco Star Ltd. as a Microwave Circuit Designer. From 1997 to 1999, he held a position of Analog Designer in Spamex N.V. in Antwerpen, Belgium. In 1999, he joined Sky Gate Ltd. in Sofia, Bulgaria, where he is currently Head of Microwave Design Department. His research interests include microwave and RF devices for phased array antennas and high-speed digital terminals.